Expected Seasonal Excitations of Earth Rotation by Unmodeled Geophysical Fluids

Yoshimitsu MASAKI

Abstract

We compare modeled (atmospheric and oceanic) seasonal excitations of the Earth rotation with the observed ones and estimate expected seasonal excitations from unmodeled geophysical fluids, primarily attributable to the hydrologic excitations. Through budget analysis of the seasonal excitations, maximum deficits in geophysical excitations occur in boreal spring to summer. If we assume a mass source on the Earth to compensate the deficits, a positive mass excess is expected around longitudes 90°E to 120°E or from 60°W to 90°W. Observation of the Earth rotation is useful for constraining geophysical excitations with some errors. The interannual variability in seasonal excitations also affects the estimation of Chandler parameters.

1. Introduction

The time-varying rotation of the Earth has been observed using optical telescopes for more than a century. Nowadays, optical telescopes have been replaced by modern space geodetic techniques, such as very long baseline interferometry (VLBI) and satellite laser ranging (SLR). The polar motion (the change in the Earth's orientation at periods longer than two days with respect to the celestial reference frame) and non-uniform change rate in Universal Time 1 (UT1, the Earth's rotation angle) are mainly excited by geophysical fluids such as the atmosphere, oceans, land water, and so on, because their distribution on the Earth changes the Earth's moment of inertia and their motion relative to the solid Earth changes the Earth's angular momentum. Since these fluids show seasonal variations, seasonal variations can also be observed in the Earth rotation data. The annually excited polar motion is called the annual wobble.

Today, several sets of geophysical fluid databases are available for academic use through the Internet. These data sets are also utilized in Earth rotation studies. For example, in terms of atmospheric data, three reanalysis data sets are widely used in meteorological studies: they are the NCEP/NCAR, NCEP-DOE and ERA-40 data. Regarding oceanic data, the ECCO project provides analysis data sets for the past 20 years. However, even though large excitations from the hydrosphere (land water, glaciers, etc.) are expected (e.g., Chen et al., 2000), currently available hydrological data sets still have large discrepancies between them and their accuracy needs to be improved.

In this paper, we estimate seasonal excitations from unmodeled geophysical fluids through budget analysis of seasonal excitations: that is, we constrain ranges of the unmodeled geophysical excitations from the geodetic observations. If we subtract the known seasonal excitations modeled by the atmospheric and oceanic data from the observed seasonal excitations, the residues give the 'unmodeled' excitations. We expect the unmodeled seasonal excitations to be mainly attributed to hydrological excitations. Since neither the distribution of geophysical fluids nor the observed Earth rotation shows constant seasonal variations over decades, we consider that there are gradual changes in their seasonal variations. Therefore, we first check the interannual variability of their seasonal changes.

The data sets and methods used in this study are shown in Section 2. The interannual variability in modeled and observed seasonal excitations is shown in Section 3. We conduct the budget analysis of seasonal excitations and estimate seasonal excitations from unmodeled geophysical fluids in Section 4. In Section 5, we examine a topic which is related to the interannual variability of seasonal excitations. We estimate effects on the Chandler parameters assuming the presence of interannual variability in seasonal signals in the polar motion.

2. Data sets and methods

The Earth orientation parameters (EOPs) data used in this study is the International Earth Rotation and Reference Systems Service (IERS) C04 series. This data is compiled by the IERS Earth Orientation Center at the Paris Observatory from space geodetic observations collected through international collaboration. Details of this data were described by Gambis (2004). We calculate geodetic excitation from this EOP data using the discrete deconvolution scheme of Wilson (1985), with the Chandler parameters of P = 431 days and Q = 179 (Wilson and Vicente, 1990) for the polar motion.

On the other hand, the atmospheric and oceanic excitations are quantified by angular momentum functions. We evaluated atmospheric angular momentum (AAM) functions (Eubanks, 1993) from three meteorological data sets, the NCEP/NCAR, NCEP-DOE and ERA-40 reanalysis data sets, because AAM functions calculated from different meteorological data sets have different values (e.g., Aoyama and Naito, 2000; Masaki and Aoyama, 2005). Comparison between different AAM functions is useful not only for cross-checks but also for estimating potential errors in meteorological data (Rosen et al., 1987). Details of the three meteorological data sets used in this study were published by Kalnay et al. (1996), Kanamitsu et al. (2002) and Uppala et al. (2005), respectively. The vertical integration of the atmospheric column is from the surface to the 10-hPa pressure level. The oceanic angular momentum (OAM) functions are downloaded from the website of the IERS Global Geophysical Fluids Center. These OAM functions are calculated from the ECCO circulation model. For details, see Gross et al. (2003, 2004).

We extract seasonal (annual and semiannual) signals by fitting sinusoids by the least-squares method. That is, the annual and semiannual signals are

$$(amplitude)\times\cos(2\pi t-(phase))$$

and

$$(amplitude)\times\cos(4\pi t-(phase)),$$

where t means time measured in units of year. In order to permit gradual changes in seasonal signals, we determine seasonal signals, using a sliding window, from every seven-year sub-sector of the entire period, 1980–2001. Note that, in Section 5, we also extract non-seasonal signals from the polar motion data, assuming that the seasonal signals are gradually changing with time. That is, we synthesize the seasonal signals from theoretical values given by the above equations at the center time of the window. Hereafter, we call this method VAVP (because we permit seasonal signals that have varying amplitudes and varying phases over the entire period). The schematic concept of this method is shown in Fig. 1.

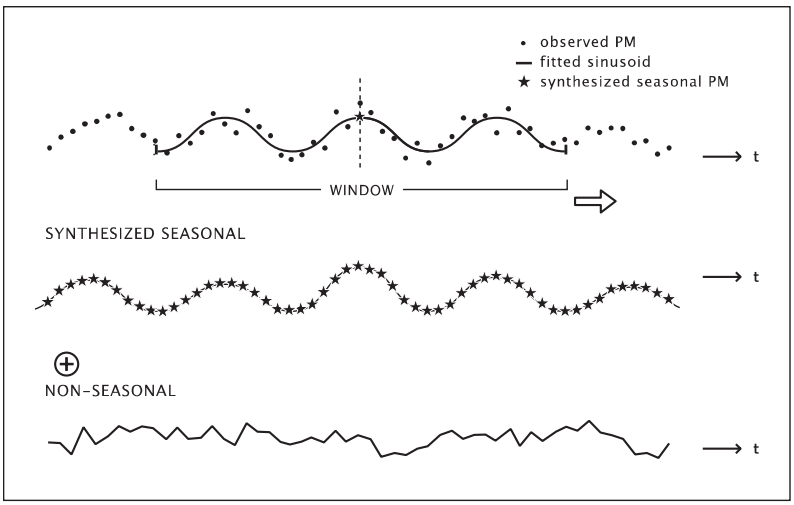

Fig. 1 Schematic concept of the VAVP method (sliding time window). In order to determine seasonal (annual and semiannual) signals, we fit sinusoids to the time-series data.

Hereafter, we introduce the Cartesian coordinate system such that the 1-axis points toward the Greenwich meridian in the equatorial plane, the 2-axis points toward 90°E in the equatorial plane and the 3-axis points toward the North Pole. The excitation vector is decomposed into these three components which are expressed as Chi-1, Chi-2 and Chi-3, respectively. Then, the equatorial excitations which drive the polar motion are expressed by a set of the (Chi-1, Chi-2) components, and the axial excitations which change the Earth's spin rate are expressed by the Chi-3 component. In this paper, we use non-dimensional units for excitations, which we can convert into familiar units by the following relations: Excitation of 1×10^{-7} for the Chi-1 or Chi-2 component corresponds to 20.6 milli-arcseconds (mas) and excitation of 1×10^{-7} for the Chi-3 component corresponds to 8.64 ms.

3. Observed and modeled seasonal excitations

First, we evaluate the observed and modeled (atmospheric and oceanic) seasonal excitations with their interannual variability.

The observed seasonal (annual and semiannual) signals are shown by red lines in Figs. 2 and 3. The annual and semiannual amplitudes show gradual changes with year. For the Chi-2 component, the annual signal becomes smaller in around 1990 and then becomes larger again at the end of the period. For the Chi-3 component, the amplitude and phase are relatively stable over the period.

The seasonal signals of the three sets of atmospheric and oceanic excitations are superimposed on Figs. 2 and 3. The geophysical excitations also show gradual changes with year and have similar interannual variations to the observed excitations, but they do not necessarily change in synchronization with the observed excitations, especially for the Chi-1 annual component. The discrepancies between different AAM functions in the interannual changes of seasonal signals are also eminent in the equatorial components.

Although each individual fluid cannot excite the observed Earth rotation, if we sum up both the atmospheric and oceanic excitations, their interannual variations show much better agreement with the observed variation. This result shows that gradual changes in the geodetic excitation are explained by these two fluids to some extent. However, differences between the observed and modeled excitations still exist, especially for the Chi-1 component. Although not shown in the figures, the atmospheric interannual variability is larger than the oceanic one.

We summarized the observed and modeled annual excitations for the first and last seven years in Table 1. For the modeled excitations, contributions from the matter term (i.e., pressure) and the motion term (i.e., winds or currents) are also indicated. The matter term dominates in power, whereas the motion term plays a significant role in the interannual variability of annual signals.

4. Expected hydrological excitations through budget analysis

In this section, we place constraints on hydrological excitations from the observed excitations, rather than estimating the hydrological excitations from doubtful hydrological data sets.

As we saw in the previous section, there are differences between the observed and modeled seasonal excitations, especially in the equatorial excitations: these differences are primarily attributed to seasonal excitations from unmodeled geophysical fluids. There are several possible sources of these deficits in the geophysical excitations, however, among them, hydrological excitations are expected to make the largest contributions to the deficits. Some pioneering researchers pointed out that hydrological excitations are very large in seasonal bands (e.g., Chao, 1988; Chen et al., 2000). Nevertheless, accurate estimation of hydrological excitations is very difficult due to the lack of hydrological observation data. Therefore, the quality of available hydrological data sets is still doubtful because there are large discrepancies between these data sets. Constructing hydrological data largely relies on climate models or climate values. In this study, so far, we excluded the hydrological data from the modeled geophysical excitations.

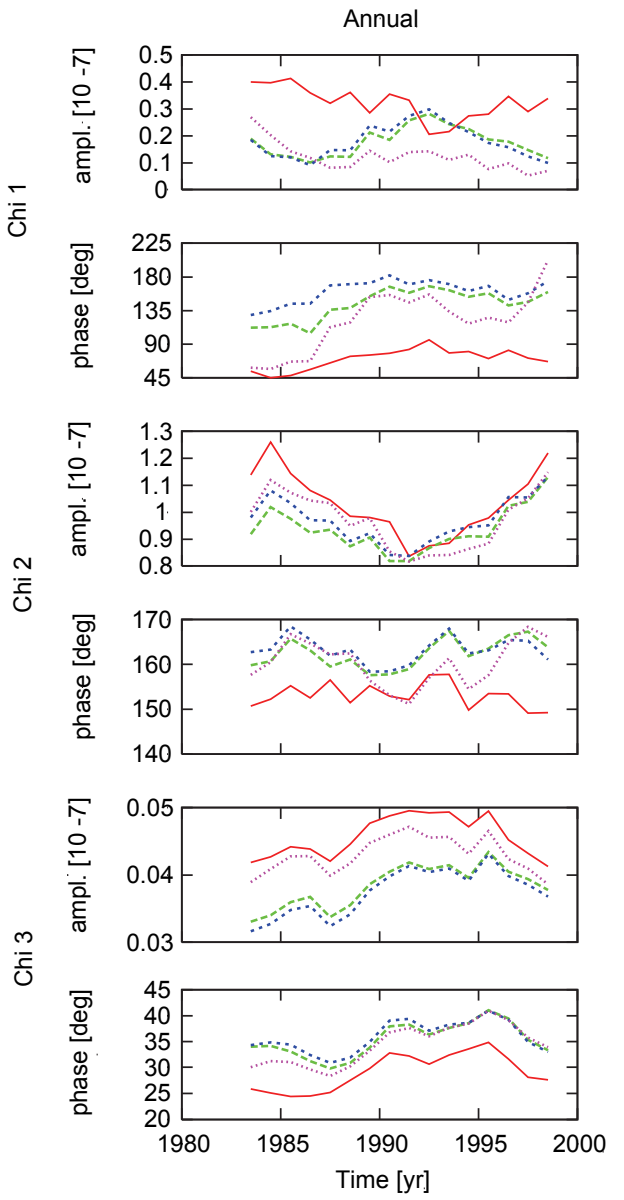

Fig. 2 Interannual variations of the observed (red solid line) and modeled (atmospheric and oceanic, broken lines) annual excitations. Annual amplitudes and phases for three components are indicated in each panel. Since we evaluated three AAM functions from different meteorological data sets, the NCEP/NCAR (green), NCEP-DOE (blue) and ERA-40 (purple) data sets, we plot the three sets of the atmospheric and oceanic excitations in the panels.

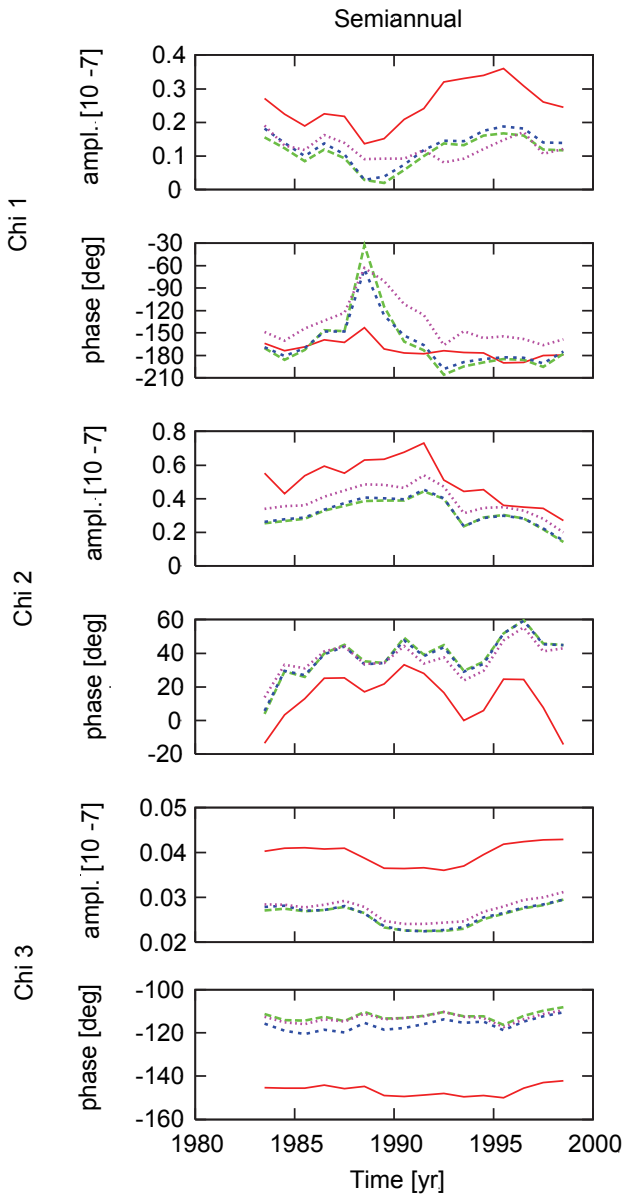

Fig. 3 Interannual variations of the observed and modeled (atmospheric and oceanic) semiannual excitations. See also the caption of Fig. 2.

Table 1 Annual signals of the observed and modeled excitations of the Earth rotation for the first (1980–1986) and last (1995–2001) seven years of the entire analysis period (1980–2001). "obp" means ocean bottom pressure.

Axis	Item	Term	1980–1986		1995–2001	
			amp. 10^{-7}	phase deg	amp. 10^{-7}	phase deg
Chi 1	geodetic excitation		0.4005	53.7	0.3382	66.5
	AAM (NCEP/NCAR)	pressure	0.3097	-178.7	0.3161	176.6
		wind	0.2194	38.1	0.0859	36.7
	OAM	obp	0.0272	117.7	0.0190	-22.3
		current	0.0810	17.4	0.1217	-10.6
Chi 2	geodetic excitation		1.1383	150.7	1.2199	149.3
	AAM (NCEP/NCAR)	pressure	1.3405	179.7	1.3646	175.6
		wind	0.1916	57.5	0.0464	100.8
	OAM	obp	0.3193	22.1	0.2621	32.3
		current	0.0839	19.0	0.0649	20.1
Chi 3	geodetic excitation		0.0419	25.9	0.0413	27.6
	AAM (NCEP/NCAR)	pressure	0.0063	-148.0	0.0045	-158.9
		wind	0.0418	33.7	0.0442	31.6
	OAM	obp	0.0016	-142.2	0.0011	-149.0
		current	0.0009	-151.6	0.0009	-167.6

Figure 4 shows a deficiency in geophysical seasonal excitations: that is, we subtract modeled geophysical excitations from the observed geodetic ones and then projected the residues onto the equatorial plane. We also compare three atmospheric excitations for two different periods, 1980–1986 and 1995–2001, as cross-checks on the atmospheric excitations.

The results show that the paths are highly elongated along longitude 90°E to 120°E. The maximum deficit occurs in the second quadrant (90°E to 120°E) in boreal spring to summer. Three paths for the last seven years, calculated from different atmospheric data, show higher accordance with each other than those for the first seven years.

5. Effects on estimation of the Chandler parameters with varying seasonal signals

In this section, we examine another topic which is related to the interannual variability of seasonal excitations.

The Chandler wobble is one of the most exciting research subjects in the field of Earth rotation and its excitation process is still unknown. The Chandler parameters, containing valuable information on the Earth's interior, can be estimated only from geodetic observations. The Chandler signals are retrieved from the observed polar motion data by subtracting seasonal signals (that is, the annual wobble). If we permit gradual change in seasonal signals, retrieved Chandler signals are also expected to change. In this section, we evaluate Chandler parameters from the retrieved nonseasonal signals using the VAVP method. That is, nonseasonal signals in Fig. 1 correspond to the retrieved Chandler signals. The Chandler parameters (the period P and damping factor Q) are estimated using the method of Jeffrey (1968).

Our results show that the estimated Chandler parameters for a constant seasonal signal are P = 432.5 days and Q = 142.6, while those for a non-constant seasonal signal are P = 432.9 days and Q = 644.3.

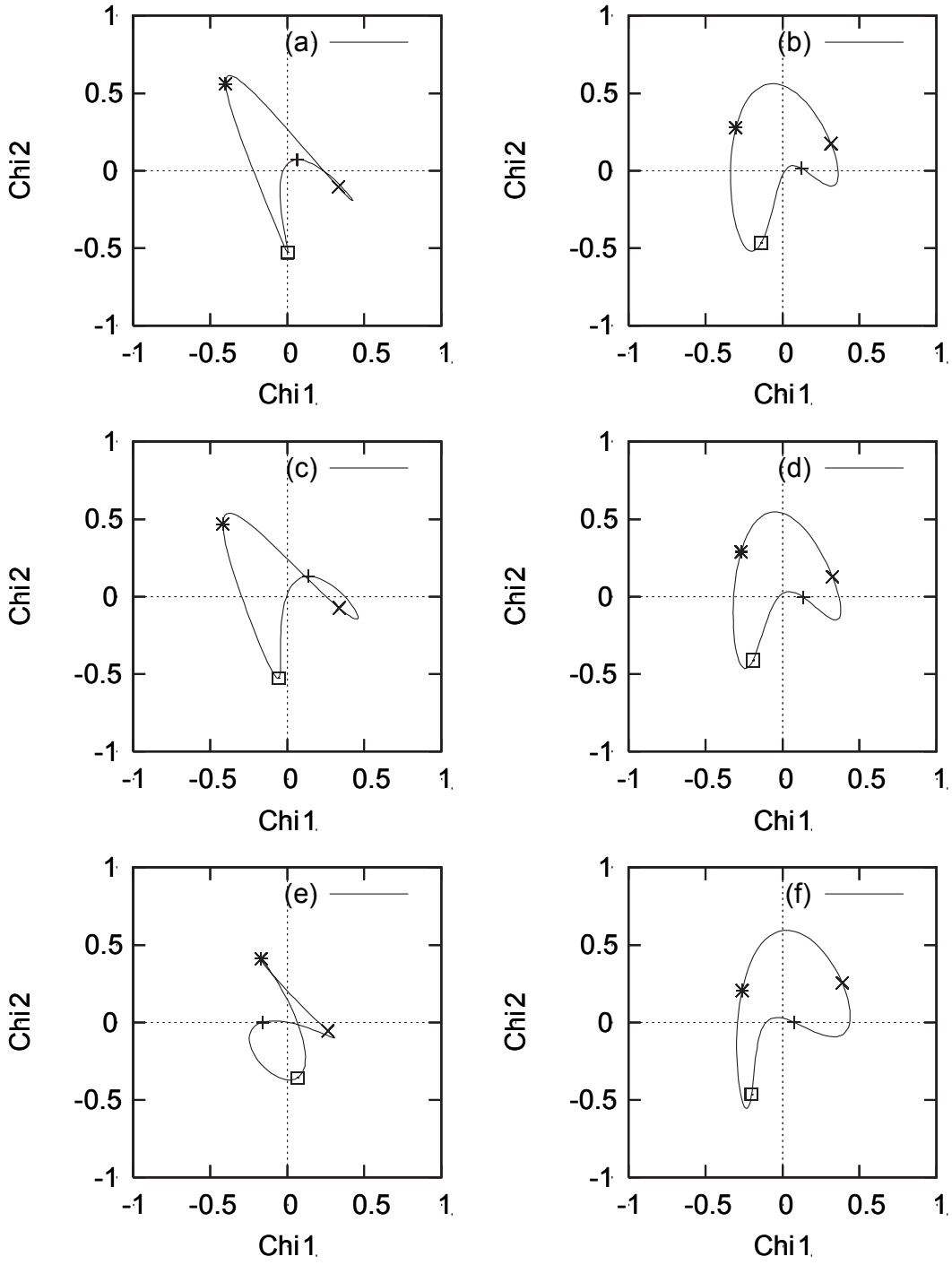

Fig. 4 The seasonal excitation deficits in modeled geophysical excitations. We considered atmospheric and oceanic excitations as the geophysical excitations and subtracted them from the observed excitations. The paths are projected onto the equatorial (Chi1-Chi2) plane. The symbols on the seasonal path are designated values at four seasons in a year (plus: 0.00 year, cross: 0.25 year, star: 0.50 year, square: 0.75 year). The atmospheric excitations are calculated from (a)(b) the NCEP/NCAR, (c)(d) NCEP-DOE and (e)(f) ERA-40 reanalysis data. The seasonal OAM functions are calculated from the OAM functions by Gross et al. (2003, 2004), based on the ECCO circulation model. We compare the results for two periods: (a)(c)(e) for the period of 1980–1986 and (b)(d)(f) for the period of 1995–2001. Units are 10^{-7}.

6. Discussion

As shown in Fig. 4, excitations of the polar motion by unmodeled geophysical fluids, which are expected to be largely attributable to the hydrosphere, show strong seasonality. We assume that unmodeled excitations are induced by mass redistribution of unmodeled geophysical fluids. Since no geophysical fluid other than the atmosphere (winds) or the ocean (currents) moves so fast on the Earth that it has large angular momentum or affects the Earth rotation, this supposition is appropriate. Then, its seasonal excitation paths projected onto the equatorial plane indicate longitudinal inhomogeneity of the seasonal mass distribution of the unmodeled fluids. The largest seasonal change in hydrological mass is expected to occur along the elongated direction of the seasonal excitation path.

As we saw in Fig. 4, large unmodeled excitations occur in boreal spring to summer (0.25 to 0.50 in fractional year) in the second quadrant on the equatorial plane and their maximum axes are oriented toward longitude 90°E to 120°E. The results indicate that, if positive mass concentration occurs at a point on the Earth, its center is located along longitude around 90°E to 120°E or 90°W to 60°W.

The hydrological mass distribution has now been clarified by the satellite gravity mission, GRACE (Tapley et al., 2004a). These twin satellites revolving around the Earth can detect the seasonal changes in gravity on the Earth. The first results of the GRACE mission revealed large seasonal variability in the local gravity field over Latin America, monsoon Asia, and so on (e.g. (Tapley et al., 2004b), accompanied by hydrological mass change. The large positive mass concentration in April over the Amazon in Latin America (~60°W) is in agreement with our results on seasonal excitation deficits. Further inspection is required to determine whether the integral effects of seasonal hydrological mass change over the Earth can explain the seasonal excitation deficits.

On the other hand, the errors in the modeled geophysical fluids also affect the budget analysis. One possible error source is atmospheric excitation from the top layer. Because we truncate the vertical integration of the atmospheric column at the 10-hPa pressure level in this study, the seasonal atmospheric excitations from 10 hPa and upper levels are not taken into account. If we evaluate the truncation errors from the atmospheric layer from 10 to 1 hPa using the ERA-40 reanalysis, their annual amplitude and phase are (0.0241×10^{-7}, 33.0°) for Chi-1 and (0.0614×10^{-7}, -137.8^{o}) for Chi-2. The semiannual amplitude and phase of the truncation errors are (0.0974×10^{-7}, -67.5^{o}) for Chi-1 and (0.0283×10^{-7}, 157.2^{o}) for Chi-2, respectively, generating much larger truncation errors than the annual ones do. These errors are much smaller than the seasonal excitation deficits shown in Fig. 4. Therefore, the truncation errors may affect the deficits but only slightly distort their path.

The potential errors in the geophysical fluids data are hard to evaluate because each data set has both merits and demerits. In practice, discrepancies in data between different data sets provide information on their quality (Rosen et al., 1987). Judging from the results in Fig. 4, we consider that the atmospheric data for the first seven years contains larger potential errors, but that the data for the last seven years contains smaller potential errors. The quality of the oceanic excitations is still under discussion, however, seasonal OAM functions are much smaller than seasonal AAM functions as shown in Table 1. We speculate that errors in OAM functions have much smaller effects on the Earth rotation excitations.

The Chandler parameters contain information on physical properties inside the Earth. The damping factor Q determined from the residual signal after removing the non-constant seasonal signal is larger than that determined from the residual signal after removing the constant seasonal signal. This is because the VAVP method tends to make the Chandler signal a regular sinusoidal variation. Because uncertainties of these parameters are large, especially for those of the damping factor Q, it is difficult to judge which result is superior. However, we showed in this paper that these parameters are easily affected by our assumption regarding the seasonal signals.

7. Conclusion

We compared the interannual variability of the observed and geophysical seasonal excitations of the Earth rotation. Both seasonal excitations show interannual changes over the past 20 years, however, discrepancies between atmospheric excitations calculated from different data sets are larger in the earlier data, possibly due to errors in the atmospheric data. Interannual variability of the observed geodetic excitations also affects the estimation of Chandler parameters.

We constrained the magnitude of unmodeled geophysical excitations other than those from the atmosphere and the oceans. Budget analysis of the seasonal excitations revealed that large deficits in geophysical excitations in boreal spring to summer exist along longitude 90°E to 120°E. A positive mass excess of the unmodeled fluids, which is expected to be due to the hydrological substance, is centered at around longitude 90°E to 120°E or 60°W to 90°W. These results agree with those on the recent seasonal mass redistribution obtained by the satellite gravity mission, GRACE. However, further inspection is required to confirm whether excitation deficits are attributed only to the hydrosphere.

In the past decade, several data sets on geophysical fluids have been constructed and made available to the public, and have assisted Earth science studies. However, the quality of the data is still not known. The Earth rotation data measured with space geodetic techniques can constrain uncertainty in geophysical fluids data. Since such fluids largely affect the Earth's climate, the Earth rotation observations collected through international collaboration will become increasingly important.

Acknowledgement

This study was financially supported by the Ministry of Education, Culture, Sports and Technology (MEXT) of Japan under a grant for Supporting Young Researchers with Fixed-term Appointments, Special Coordination Funds for Promoting Science and Technology.

The EOPs and the oceanic excitations used in this study were downloaded from the IERS EOP Center and the IERS Global Geophysical Fluid Center. The NCEP/NCAR and NCEP-DOE reanalysis data sets were downloaded from the respective websites.

References

Aoyama, Y. and I. Naito (2000): Wind Contributions to the Earth's Angular Momentum Budgets in Seasonal Variation, Journal of Geophysical Research, 105 (D10), 12417–12431.

Chao, B.F. (1988): Excitation of the Earth's Polar Motion due to Mass Variations in Major Hydrological Reservoirs, Journal of Geophysical Research, 93 (B11), 13811–13819.

Chen, J.L., C.R. Wilson, B.F. Chao, C.K. Shum and B.D. Tapley (2000): Hydrological and Oceanic Excitations to Polar Motion and Length-of-day Variation, Geophysical Journal International, 141, 149–156.

Eubanks, T.M. (1993): Variations in the Orientation of the Earth, in Contributions of Space Geodesy to Geodynamics: Earth Dynamics, D.E. Smith and D.L. Turcotte (eds.), Geodynamics Series 24, American Geophysical Union, Washington D.C., 1–54.

Gambis, D. (2004): Monitoring Earth Orientation using Space-geodetic Techniques: State-of-the-art and Prospective, Journal of Geodesy, 78, 295–303.

Gross, R.S., I. Fukumori and D. Menemenlis (2003): Atmospheric and Oceanic Excitation of the Earth's Wobbles during 1980–2000, Journal of Geophysical Research, 108 (B8), 2370, doi: 10.1029/2002JB002143.

Gross, R.S., I. Fukumori and D. Menemenlis (2004): Atmospheric and Oceanic Excitation of Length-of-day Variations during 1980–2000, Journal of Geophysical Research, 109, B01406, doi: 10.1029/2003JB002432.

Jeffreys, H. (1968): The Variation of Latitude, Monthly Notices of the Royal Astronomical Society, 141, 255–268.

Kalnay, E., M. Kanamitsu, R. Kistler, W. Collins, D. Deaven, L. Gandin, M. Iredell, S. Saha, G. White, J. Woollen, Y. Zhu, M. Chelliah, W. Ebisuzaki, W. Higgins, J. Janowiak, K.C. Mo, C. Ropelewski, J.

Wang, A. Leetmaa, R. Reynolds, R. Jenne and D. Joseph (1996): The NCEP/NCAR 40-Year Reanalysis Project, Bulletin of the American Meteorological Society, 77 (3), 437–471.

Kanamitsu, M., W. Ebisuzaki, J. Woollen, S.-K. Yang, J.J. Hnilo, M. Fiorino and G.L. Potter (2002): NCEP-DOE AMIP-II Reanalysis (R-2), Bulletin of the American Meteorological Society, 83 (11), 1631–1643.

Masaki, Y. and Y. Aoyama (2005): Seasonal and non-seasonal AAM functions from different reanalysis data sets, in Proceedings of Forcing of Polar Motion in the Chandler Frequency Band: A Contribution to Understanding Interannual Climate Variation (H.-P. Plag et al. eds.), Cahiers du Centre Européen de Géodynamique et de Séismologie, 24, Luxembourg, 103–108.

Rosen, R.D., D.A. Salstein, A.J. Miller and K. Arpe (1987): Accuracy of Atmospheric Angular Momentum Estimates from Operational Analyses, Monthly Weather Review, 115, 1627–1639.

Tapley, B.D., S. Bettadpur, J.C. Ries, P.F. Thompson and M.M. Watkins (2004a): GRACE Measurements of Mass Variability in the Earth System, Science, 305, 503–505.

Tapley, B.D., S. Bettadpur, M. Watkins and C. Reigber (2004b): The Gravity Recovery and Climate Experiment: Mission Overview and Early Results, Geophysical Research Letters, 31, L09607, doi: 10.1029/2004GL019920.

Uppala, S.M., P.W. Kållberg, A.J. Simmons, U. Andrae, V. Da Costa Bechtold, M. Fiorino, J.K. Gibson, J. Haseler, A. Hernandez, G.A. Kelly, X. Li, K. Onogi, S. Saarinen, N. Sokka, R.P. Allan, E. Andersson, K. Arpe, M.A. Balmaseda, A.C.M. Beljaars, L. Van de Berg, J. Bidlot, N. Bormann, S. Caires, F. Chevallier, A. Dethof, M. Dragosavac, M. Fisher, M. Fuentes, S. Hagemann, E. Hólm, B.J. Hoskins, L. Isaksen, P.A.E.M. Janssen, R. Jenne, A.P. McNally, J.-F. Mahfouf, J.-J. Morcrette, N.A. Rayner, R.W. Saunders, P. Simon, A. Sterl, K.E. Trenberth, A. Untch, D. Vasiljevic, P. Viterbo and J. Woollen (2005): The ERA-40 Re-analysis, Quarterly Journal of the Royal Meteorological Society, 131, 2961–3012.

Wilson, C.R. (1985): Discrete Polar Motion Equations, Geophysical Journal of the Royal Astronomical Society, 80, 551–554.

Wilson, C.R. and R.O. Vicente (1990): Maximum likelihood estimates of polar motion parameters, Variations in Earth Rotation, Geophysics Monograph Series, 59, (D.D. McCarthy and W.E. Carter, eds.), 151–155, AGU, Washington D.C.